# Characterization of a hydrogen flame as an ion source for mass spectrometry

JAAS Journal of Analytical Atomic Spectrometry

**Lee L. Yu,* Gregory C. Turk and S. Roy Koirtyohann†**

*Analytical Chemistry Division, National Institute of Standards and Technology, Gaithersburg, MD 20899, USA*

***Received 16th December 1998, Accepted 16th December 1998***

A commercial inductively coupled plasma (ICP) mass spectrometer was modified to employ an air–hydrogen flame in place of the ICP as an ion source. A liquid nitrogen trap was placed in the vacuum line to remove water. A very simple intrinsic mass spectral background was obtained with the hydrogen flame ionization mass spectrometry (FIMS). Molecular ions such as $K(H_2O)^+$, $Na(H_2O)^+$, $Ca(H_2O)^+$ and $CaOH(H_2O)_x^+$ ($x=0$–2) were observed when solutions containing Na, K or Ca were aspirated. Although the presence of the molecular ions complicated the mass spectra, it also provided a wider choice of analytical masses for an analyte. Isotope ratio measurements of Ca were made with both $Ca^+$ and $CaOH^+$ species at masses 40, 44, 57 and 61. Better isotope ratio precision was obtained at $CaOH^+$ masses relative to those for $Ca^+$ because the sensitivity was about 10 times higher. Isotope ratio measurement of K was made at masses 39 and 41. A ratio precision of about 0.2 and 0.5% was obtained for K and Ca, respectively. The results suggest that the FIMS is suitable for the isotope ratio measurement of K and Ca in simple matrices, and that the air–hydrogen flame is a more desirable ion source than an air–acetylene flame for FIMS.

## Introduction

The spectral background of inductively coupled plasma mass spectrometry (ICP-MS) has been well documented.[1,2] While many interferences from the plasma background can be minimized by desolvation[3,4] or by using an Ar–$N_2$ mixed gas plasma,[5,6] solutions to the interferences from $Ar^+$ are surprisingly few. As a result, isotope ratio measurements of K and Ca are severely impaired. One approach that has gained limited success is to minimize the amount of $Ar^+$ being extracted by the mass spectrometer. In this effort, Smith *et al.*[7] used an Ar–Xe supported plasma and a high resolution mode of the mass spectrometer. The background at mass 40 was greatly reduced and its effect on K masses was minimized. The interference of $^{38}ArH^+$ at mass 39 was negligible; nevertheless, the $^{40}ArH^+$ interference at mass 41 was still the equivalent of about 0.9 ppm K. Despite the $^{40}ArH^+$ background, the measured K isotope ratio was reasonably close to the accepted value.[7]

Jiang *et al.*[8] virtually eliminated the $Ar^+$ and $ArH^+$ species in the spectral background by operating an ICP-MS under cool plasma conditions. A detailed study of the 'cold plasma' conditions by Tanner[9] showed that interferences from $Ar^+$ were minimized whereas those from $ArH^+$ persisted. A non-linear relationship was observed between the count rate and the concentration of K, but the non-linearity was not expected to affect the isotope ratio measurements.[8] A 9% mass bias was observed for the $^{39}K/^{41}K$ ratio.[8] Despite the fact that the count rate for $^{39}K^+$ was lowered by about two orders of magnitude, the detection limit was similar to that obtainable with conventional instrument settings.[8] Argon ions are an integral part of energy transfer to the plasma; therefore, their populations cannot be dramatically reduced without extinguishing the plasma.

Replacing the plasma with a different ion source is another possible solution to the background problem. Zhang *et al.*[10,11] developed a helium inductively coupled plasma mass spectrometer. Elements such as K and Fe that suffer from spectral interferences in Ar ICP-MS were detected at 0.1 and 4 pg $mL^{-1}$, respectively. Mass spectrometers were extensively used to study the molecular species in the combustion flame in order to elucidate the combustion mechanism.[12–14] Conversely, flames can serve as alternative ion sources to the plasma for elemental mass spectrometry. Taylor *et al.*[15] used an air–acetylene flame to this effect. A lower detection limit of K was reported in comparison with that obtained by ICP-MS. Isotope ratio measurements of K were made, and the feasibility of flame ionization mass spectrometry (FIMS) for ground water studies by using $^{41}K$ as a stable tracer was demonstrated. Unfortunately, the organic combustion products of an acetylene flame resulted in instrument contamination. A significant amount of a wax-like residue was observed inside the interface of the instrument after several hours of operation. It is likely that this accumulation has a deleterious effect on instrument performance, making an air–acetylene flame less suitable as an ion source. Alternatively, an air–hydrogen flame can be used for mass spectrometry, as reported by Turk *et al.*[16] Unlike the residue from an acetylene flame, the water resulting from combustion was easily removed from the vacuum system with a liquid nitrogen trap.[16] In that work,[16] the flame was used as an atom source and ionization of ground state analyte atoms was accomplished by laser-enhanced ionization (LEI) with subsequent mass spectrometric detection. At a temperature of about 2300K,[17] an air–hydrogen flame is capable of ionizing most of the alkali and alkaline earth elements to a significant degree.[18] Therefore, it can also be an effective ion source for these elements.

†Present address: Department of Chemistry, University of Missouri at Columbia, Columbia, MO 65211, USA.

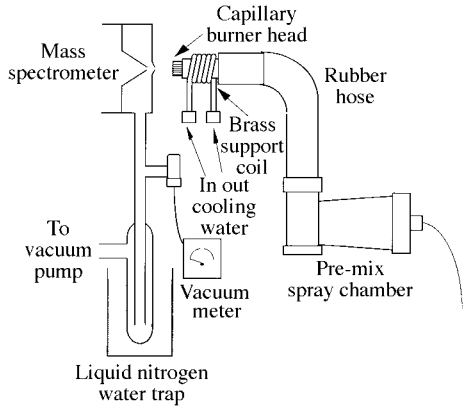


**Fig. 1** Schematic diagram of a hydrogen burner and MS interface.

**Table 1** Instrument parameters

| | |
|---|---|
| Mass spectrometer | Perkin-Elmer SCIEX Elan 5000 |
| Spectral resolution | 0.8 u (normal) |
| Sample uptake rate | 0.94 mL $min^{-1}$ |
| Ni sampler and Ni skimmer orifice diameter | 0.5 mm |
| Spacing between the burner and the sampler | 20 mm |
| Interface pressure | 230 Pa (1.7 Torr) |
| Quadrupole pressure | 2.9 mPa ($2.2 \times 10^{-5}$ Torr) |

## Experimental

### Reagents and equipment‡

An Elan 5000 ICP-MS (Perkin-Elmer SCIEX, Thornhill, Ontario, Canada) and a pre-mix burner and nebulization system designed for flame atomic absorption spectrometry from Perkin-Elmer (Norwalk, CT, USA) were adapted for this work. A schematic diagram of the FIMS is shown in Fig. 1. Model 604 and 603 tapered rotameter flow meters from Matheson Gas Products (Secaucus, NJ, USA) were used to control the flows of the air and the hydrogen, respectively. A capillary burner head was used rather than the normal slot-type burner head. It was constructed with a bundle of 43, 4 cm × 1 mm id stainless steel capillaries clustered into 1 cm diameter and mounted in a water-cooled holder in the position where the ICP torch normally is located. The burner head was connected to the spray chamber with a 3 cm id flexible hose. A Gilson (Middleton, WI, USA) peristaltic pump was used to regulate the sample uptake. The vacuum pressure of the instrument was maintained by decreasing the orifice of both the sampler and the skimmer to 0.5 mm, and by increasing the pumping capacity by using a RUVAC WAU-250 Roots blower from Leybold Vacuum Products (Export, PA, USA) in series with the instrument roughing pump. Water was removed from the vacuum line by a Reliance Glass Works (Bensenville, IL, USA) Model R-7210 liquid nitrogen trap installed upstream of the Roots blower. A Convectron Model 275 vacuum gauge from Granville-Phillips (Boulder, CO, USA) was also installed to monitor the pressure in the interface region. Control over the interlocks of the mass spectrometer was achieved by using the service mode of the Elantools software. Table 1 gives the instrument parameters used.

All standard solutions were prepared by appropriate dilutions of 3100 Series Standard Reference Materials from the National Institute of Standards and Technology (Gaithersburg, MD, USA) in 0.2 M $HNO_3$ prepared locally by sub-boiling distillation. Sample solutions contained a similar acid concentration.

‡Certain commercial instruments are identified in this paper to specify adequately the experimental procedure. Such identification does not imply recommendation or endorsement by the National Institute of Standards and Technology, nor does it imply that the equipment identified is necessarily the best for the purpose.

### Procedure

An air–hydrogen flame was used for all the elements studied except Ca, for which an oxygen-enriched air–hydrogen flame was used. The gas flow rates for the air–hydrogen flame were 4.3 L $min^{-1}$ for air and 3.7 L $min^{-1}$ for hydrogen. For the spectral background studies, a mass scan consisting of six sweeps over the entire mass range (1–250 u) was performed with a blank solution. The total dwell time at each mass was 1.8 s. For the molecular ion studies, four single element solutions containing 100 ppm Na, 10 ppm K, 40 ppm Ca and 10 ppm Fe were used. Mass scans from 39 to 97 u were performed for each solution.

A calibration curve for K was constructed using solutions containing 0, 0.078, 0.38, 1.9, 9.3, 31 and 100 ppm K. For K isotope ratio measurements, five replicate measurements were made on solutions containing 32 and 100 ppm K. The total dwell time for each measurement was 36 and 144 s at masses 39 and 41, respectively.

An oxygen-enriched air–hydrogen flame was used for the studies on Ca. The flow of the oxygen was regulated using the oxygen channel of the mass flow controller of the ELAN 5000 ICP-MS. The oxygen entered the burner through the auxiliary oxidant port of the spray chamber. Typical flow rates were 0.20 L $min^{-1}$ of $O_2$, 3.6 L $min^{-1}$ of air and 4.6 L $min^{-1}$ of $H_2$. A calibration curve for Ca was constructed with solutions containing 0, 1.0, 2.0, 2.7, 3.9, 4.9, 6.5, 8.4, 9.3, 11, 23, 32 and 40 ppm Ca. Isotope ratio measurements were made using 10 replicates of a 40 ppm Ca solution. The total dwell time for each measurement was 5, 35, 5 and 35 s at masses 40, 44, 57 and 61, respectively. For studies of ionization interferences, a blank and five samples were prepared. The five samples contained 10 ppm Ca, 10 ppm K, 10 ppm K plus 10 ppm Ca, 100 ppm Na and 100 ppm Na plus 10 ppm Ca. The count rates at masses 40, 44, 57 and 61 were measured.

The detection limit was determined as the concentration giving a signal equivalent to three times the noise, calculated from the standard deviation of 11 repetitive measurements with 3 s integration of the background intensity.

## Results and discussion

### General properties of the hydrogen FIMS

When a commercial ICP-MS instrument is retrofitted with a sampler of a smaller orifice, the geometry of the supersonic jet changes. It is important to ensure that the skimmer is within the boundary of the Mach disk to minimize interactions that could alter the chemical composition of the sample extracted from the ion source.[14] Some researchers have suggested that the optimum sampler–skimmer separation for an Ar plasma ion source is two thirds of the Mach disk location relative to the sampler.[19] The position of the Mach disk was calculated[19] using the measured interface pressure (see Table 1) and the diameter of the sampler orifice. This calculation places the location of the Mach disk approximately 7 mm behind the orifice. Therefore, the skimmer, which was about 6.1 mm from the sampler orifice, was inside the Mach disk.

The mass spectrum of a 0.2 M nitric acid solution is shown in Fig. 2. The $H_3O^+$, $CH_2O^+$, $NO^+$ and $NO_2H^+$ peaks found in the background spectrum of an acetylene FIMS were not observed in the hydrogen FIMS.[15] The temperature of an air–hydrogen flame is about 150 K lower than that of an air–acetylene flame.[17] The lower temperature and a lack of flame carbon relative to the air–acetylene flame are probably

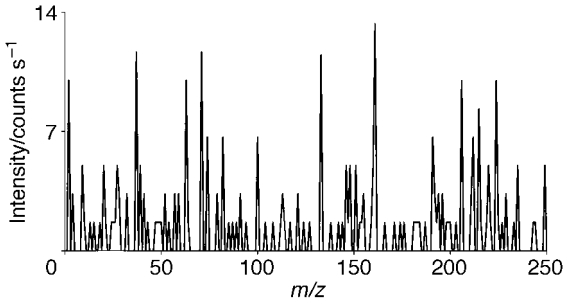


**Fig. 2** Mass spectral background of a blank containing 0.2 M nitric acid.

directly or indirectly[20] responsible for the absence of these background species. The background intensity of the hydrogen FIMS at any mass was below 14 counts s$^{-1}$. Data from the six replicates of a scan showed that the average of the intensities at any given mass was smaller than the standard deviation of the intensities at the mass, suggesting that the features observed in the background scan were due primary to statistical noise. The hydrogen flame is, therefore, a clean source for mass spectrometry.

The signal intensity of a 10 ppm K solution was about $9 \times 10^4$ counts s$^{-1}$ at mass 39, yielding a sensitivity of 350 counts s$^{-1}$ μM$^{-1}$. With some reasonable assumptions, the sensitivity and hence the efficacy of the FIMS for the other elements can be estimated by using the ionization potential of the analyte. The ion number density in the hydrogen flame is related to the ionization potential of the element by the Saha equation:[21]

$$\log \frac{[M^+]^2}{[M]} = -5040 \frac{V_i}{T} + 2.5 \log T - 6.5 \quad (1)$$

where $[M^+]$ and $[M]$ are the ion and atom number densities, respectively, of the analyte, $V_i$ is the ionization potential of the analyte in electronvolts and $T$ is the flame temperature (2300 K). The mass spectrometric signal intensity is directly proportional to the ion number density of the isotope:

$$[M^+] = kI \quad (2)$$

where $I$ is the signal intensity and $k$ is the FIMS response constant for the element. The atom number density is directly proportional to the free atom fraction of the analyte and the molarity of the analyte solution aspirated:

$$[M] = f\beta C \quad (3)$$

where $f$ is a constant of the flame, $\beta$ is the atomization factor of the analyte and $C$ is the analyte molar concentration. Let us assume that the mass response curve of the spectrometer is flat and therefore the response constant $k$ is approximately the same for all elements. Then for isotopes of element $a$ and element $b$ of the same molarity ($C_a = C_b$), the following applies:

$$\log \frac{[M_a{}^+]^2}{[M_a]} = \log \frac{(kI_a)^2}{fC_a\beta_a} = -5040 \frac{V_{ai}}{T} + 2.5 \log T - 6.5 \quad (4)$$

$$\log \frac{[M_b{}^+]^2}{[M_b]} = \log \frac{(kI_b)^2}{fC_b\beta_b} = -5040 \frac{V_{bi}}{T} + 2.5 \log T - 6.5 \quad (5)$$

Subtracting eq. (4) from eq. (5) we obtain

$$\log \frac{I_b{}^2}{I_a{}^2} = -5040 \frac{V_{bi} - V_{ai}}{T} + \log \frac{\beta_b}{\beta_a} \quad (6)$$

For isotope ratio measurements to be practical, a minimum sensitivity of 4 counts s$^{-1}$ μM$^{-1}$ [the equivalent of 100 counts s$^{-1}$ (ppm)$^{-1}$ at mass 39] is needed for an analyte. Substitute $I_a$, $V_{ai}$ and $\beta_a$ in eqn. (6) with the sensitivity of 350 counts s$^{-1}$ μM$^{-1}$, the ionization potential of 4.3 eV and atomization factor of 0.4 for K.[17] Substituting $I_b$ in eqn. (6) with the limit sensitivity of 4 counts s$^{-1}$ (ppm)$^{-1}$ and using a flame temperature of 2300 K, eqn. (6) is reduced to

$$V_{bi} = 6.3 + 0.46 \log \beta_b \quad (7)$$

The ionization potential $V_{bi}$ has a maximum of 6.3 eV since $\beta_b$ cannot be greater than 1. Hence, the usefulness of the hydrogen FIMS is limited to elements with ionization potentials below 6.3 eV, which include most of the alkali and alkaline earth elements. If the atomization factor of an analyte is less than 1, the corresponding $V_{bi}$ for the element is lowered. An example is Ca, which has an atomization factor of 0.15 in an air–hydrogen flame.[17] $V_{bi}$ for Ca is calculated to be 5.9 eV, which is less than the first ionization potential of 6.1 eV for the element. This suggests that $Ca^+$ is not sensitive enough to be useful for isotope ratio measurement with the hydrogen FIMS, and therefore the measurement of Ca has to be made with other alternatives, as will be discussed later. The limited ionization capability of the hydrogen FIMS is an advantage rather than a disadvantage for the determination of the alkali and alkaline earth elements, because it promises a simpler mass spectrum relative to that of ICP-MS for samples of complex matrices.

## Molecular ions

The primary application of the hydrogen FIMS research is the isotope ratio measurements of K and Ca for which the conventional ICP-MS technique is inadequate because of the isobaric interferences. Na and Fe are present in most sample matrices; therefore, they were included in the study. Spectra of the four elements using single element solutions are shown in Fig. 3.

The mass spectrum of a 100 ppm Na solution showed two peaks at K masses, one at mass 39 with 700 counts s$^{-1}$ and the other at mass 41 with 3000 counts s$^{-1}$ [Fig. 3(a)]. The peak at mass 39 was probably K from the contamination of the burner head after the prolonged use with high concentrations of K solutions. The more intense peak at mass 41 cannot be explained by the K contamination because of the low natural abundance of $^{41}K$. The probable designation for this peak was $Na(H_2O)^+$. The background from the molecular ions of the 100 ppm Na solution was the equivalent of about 2 ppm natural K at mass 41. A separation may be necessary for isotope ratio measurement of K in samples containing high concentrations of Na. Alternatively, the interference on $^{41}K$ may be avoided by preparing the samples in $D_2O$.

The mass scan of a 10 ppm K solution [Fig. 3(b)] showed a peak at mass 57 with 1000 counts s$^{-1}$ and another at mass 59 with 100 counts s$^{-1}$ in addition to the peaks at K masses. The probable species responsible for the peaks were the hydrated analyte ions $^{39}K(H_2O)^+$ and $^{41}K(H_2O)^+$. The intensities of $K^+$ at masses 39 and 41 were $1 \times 10^5$ and $1 \times 10^4$ counts s$^{-1}$, respectively. Assuming a flat mass response curve of the FIMS in the mass range of this study the $K^+$ species were estimated to account for over 99% of the total K containing ions.

The mass scan of a 40 ppm Ca solution [Fig. 3(c)] showed four groups of peaks in the mass range studied. The first group from masses 39 to 44 included peaks of $^{39}K^+$ as a contaminant at 900 counts s$^{-1}$, $^{40}Ca^+$ at 3000 counts s$^{-1}$ and $^{44}Ca^+$ at 80 counts s$^{-1}$. The second group included peaks from masses 57 to 65. Based on the intensities of these peaks relative to one another, the probable identifications of the peaks were $CaOH^+$ species at masses 57 (30 000 counts s$^{-1}$),

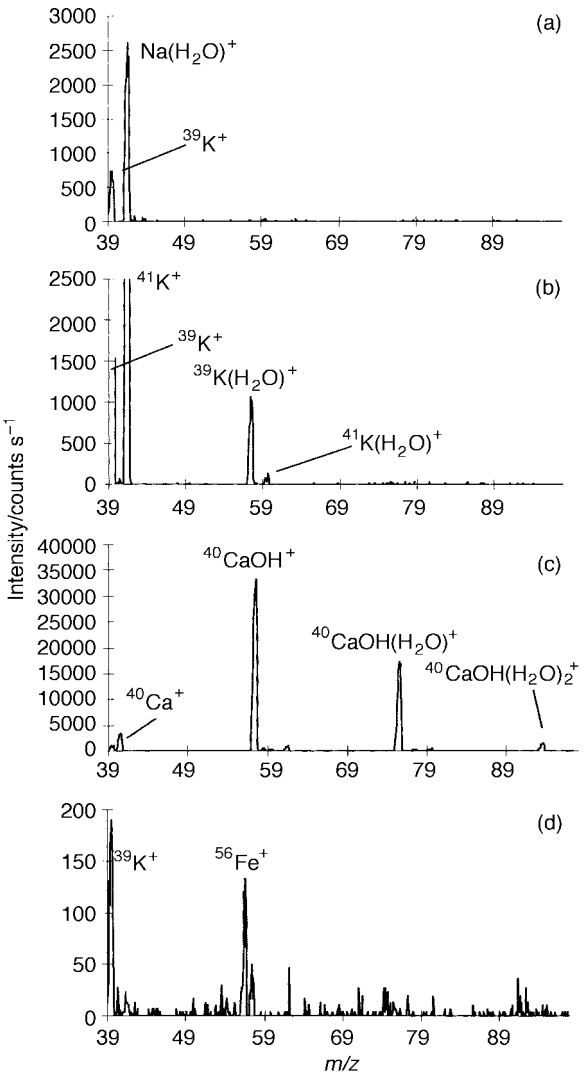


**Fig. 3** Mass spectra of (a) 100 ppm Na, (b) 10 ppm K, (c) 40 ppm Ca and (d) 10 ppm Fe.

59 (300 counts $s^{-1}$), 60 (80 counts $s^{-1}$), 61 (1000 counts $s^{-1}$) and 65 (60 counts $s^{-1}$), and $^{40}Ca(H_2O)^+$ at mass 58 (500 counts $s^{-1}$). The third group included peaks from masses 75 to 83. The probable identifications for these peaks were $CaOH(H_2O)^+$ species at masses 75 (20 000 counts $s^{-1}$), 77 (200 counts $s^{-1}$), 78 (30 counts $s^{-1}$) and 79 (300 counts $s^{-1}$) and $Ca(H_2O)_2^+$ at mass 76 (30 counts $s^{-1}$). The fourth group included peaks from masses 93 to 97. The probable identifications for these peaks were $CaOH(H_2O)_2^+$ at masses 93 (1000 counts $s^{-1}$), 95 (20 counts $s^{-1}$) and 97 (40 counts $s^{-1}$). Assuming a flat mass response curve of the FIMS, the relative abundance of the Ca species was about 55, 37, 5, 2 and 1% for $CaOH^+$, $CaOH(H_2O)^+$, $Ca^+$, $CaOH(H_2O)_2^+$ and $Ca(H_2O)^+$, respectively. Therefore, $CaOH^+$ was the dominant Ca species in the FIMS.

The spectrum of a 10 ppm Fe solution [Fig. 3(d)] showed two major peaks at masses 39 and 56, respectively. The peak at mass 39 was probably K contaminant from the burner head discussed earlier. The peak at mass 56 with an intensity of about 120 counts $s^{-1}$ was from Fe. Apparently, the high ionization potential of Fe (7.87 eV), relative to the limit of 6.3 eV discussed earlier, was responsible for the low sensitivity.

The hydrate ions observed in Na, K and Ca spectra were probably formed during the supersonic jet expansion.[22] As the gas expanded from the flame into the vacuum through the sampler orifice, its temperature dropped faster than the pressure relative to the local dew point.[22] The gas may become supersaturated at some stage of the expansion, resulting in homogeneous nucleation and the formation of the hydrate ions.[22] These hydrate ion species are rarely observed in ICP-MS, probably owing to the high temperature of the plasma and the low partial pressure of water relative to that of Ar. The presence of the hydrates of $Na^+$, $K^+$, $Ca^+$ and $CaOH^+$ complicates the mass spectra of the hydrogen FIMS. Analyte ion–solvent clusters are frequently observed[23,24] in the spectra obtained using electrospray mass spectrometry (ES-MS). The extent of the analyte ion–solvent cluster depends on the electric field strength between the sampler and the skimmer. Increasing the voltage promotes collisions in the free jet,[23] resulting in diminished hydrate ion intensities relative to singly charged analyte ions.[23,24] This de-clustering principle of ES-MS should also be applicable to the hydrogen FIMS, and the hydrate ions in the hydrogen FIMS probably could be minimized by appropriate biasing of the sampler and the skimmer. No attempt was made to do so in the present work.

### Analytical performance with potassium

Taylor *et al.*[15] reported that with an air–acetylene flame, a 100 ppm Cs solution aspirating between each sample analysis was essential to keep the K signal stable. Without the Cs solution the K signal would drift down to the background level in 10–15 min.[15] This phenomenon was not observed with the air–hydrogen flame. Calibration standards of K in 0.2 M nitric acid were measured and the intensities were plotted against the concentrations of K. A linear curve (correlation 0.9997) spanning over three orders of magnitude was indicated. The detection limit for K was about 0.2 ppb. This is comparable to the 0.2–0.3 ppb reported by Taylor *et al.*[15] using an acetylene FIMS and it is slightly better than the 1 ppb obtained with ICP-MS;[25] however, a much better detection limit of 0.1 pg $mL^{-1}$ can be obtained with helium ICP-MS.[10] Two solutions containing natural K were used for isotope ratio measurements. The mass bias calculated from the measured ratio of 13.51 was about 2.5% lower relative to the accepted ratio of 13.86, compared with the 9% bias observed in a cool plasma.[8] The results for five replicate measurements gave 0.19 and 0.14% relative standard deviation (RSD) for 32 and 100 ppm K, respectively.

A mass scan of a 1000 ppm K solution is shown in Fig. 4. The magnitudes of the three peaks at masses 39, 40 and 41 were $1.63 \times 10^6$, 238 and $1.19 \times 10^5$ counts $s^{-1}$, respectively, yielding abundances of 93, 0.014 and 6.8% (not corrected for mass bias), respectively. They were in good proportion relative to the accepted abundances of 93, 0.012 and 6.7% for the corresponding K isotopes. The fact that the peak at mass 40 is well resolved from those at 39 and 41 suggests that the measurement of $^{40}K$ is possible.

Potassium-40 is sometimes used for mineral dating.[26] The

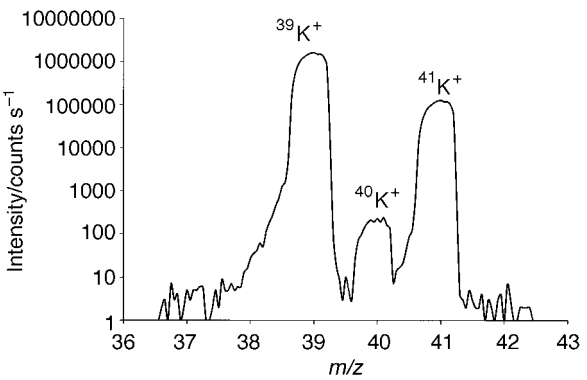


**Fig. 4** Mass spectrum of a 1000 ppm K solution.

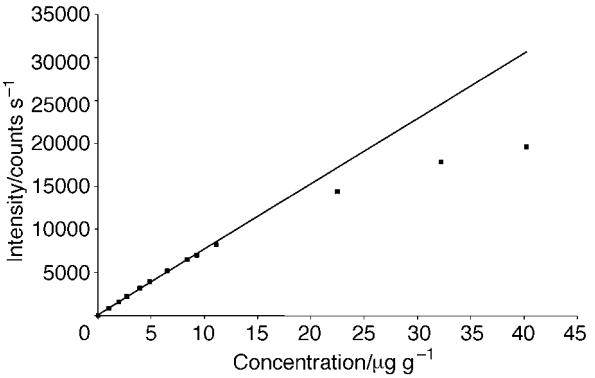


**Fig. 5** Calibration curve for Ca.

capability of the FIMS for the measurement of $^{40}$K can be compared with radiochemical scintillation counting. At the signal intensity of the experiment, it would take about 70 min to collect $10^6$ counts at mass 40. A 70 mL volume of 1000 ppm K solution would be needed with a sample uptake of 1 mL min$^{-1}$ of the current nebulizer. The sample uptake can be reduced easily without sacrificing the sensitivity or the signal stability by using a direct injection high-efficiency nebulizer (DIHEN).[27] An estimated 7 mL of the solution are needed with a sample uptake of 0.1 mL min$^{-1}$ of the DIHEN;[27] therefore, the calculated volume of 70 mL is the upper limit. The $^{40}$K in 70 mL of the solution is about $1.30 \times 10^{17}$ atoms. Assuming a 100% detector efficiency, the time it would take to collect $N$ counts is

$$t = \frac{Nt_{1/2}}{N_0 \ln 2} \quad (8)$$

where $t_{1/2}$ is the half-life of $^{40}$K ($1.27 \times 10^9$ years) and $N_0$ the number of $^{40}$K atoms in the K solution at the beginning. A simple calculation shows that with 70 mL of 1000 ppm K, scintillation counting would take over 5 d to collect the same number of counts. Therefore, the mass spectrometric method has the potential to be more practical than scintillation counting for $^{40}$K determinations.

### Analytical performance with Ca

According to the discussion on the general properties of the hydrogen FIMS, Ca has a sensitivity below the limit of 4 counts s$^{-1}$ μM$^{-1}$ [or about 100 counts s$^{-1}$ (ppm)$^{-1}$] set forth previously. A measurement of a 2.7 ppm Ca solution with the air–hydrogen FIMS gave a count rate of about 160 counts s$^{-1}$, or a sensitivity of about 60 counts s$^{-1}$ (ppm)$^{-1}$. Since the rate of ionization is exponentially proportional to the temperature of the flame, the higher the flame temperature, the higher is the sensitivity. An oxygen–hydrogen flame would be more desirable for Ca because of its higher temperature relative to an air–hydrogen flame; however, the oxygen–hydrogen flame is extremely susceptible to flash back. In this work, an oxygen enriched air–hydrogen flame was used to enhance the Ca sensitivity. As the flow of the air was decreased, the flow of the oxygen was increased, and the flow of hydrogen was also increased in order to maintain the linear flow velocity of the gas mixture. This procedure reduced the chance of a flash back. The sensitivity of Ca was increased by a factor of about 8 in the oxygen-enriched flame relative to that in the air–hydrogen flame. Fig. 5 shows the calibration curve of Ca using signal intensities at mass 40. The curve is linear up to about 10 ppm (correlation 0.9993), beyond which it bends toward the concentration axis. The curvature at concentrations higher than 10 ppm is probably a result of auto-ionization suppression, since the element is highly susceptible to ionization interferences to be discussed later. The detection limit was about 2 ppb at mass 40 compared with the 2 ppb at mass 44 by ICP-MS.[25] As discussed earlier, the sensitivity of $CaOH^+$ was about 10 times higher than that of $Ca^+$. Consequently, a better detection limit of 0.2 ppb was obtained at mass 57.

A 40 ppm Ca solution was used to demonstrate an isotope ratio measurement. Signal intensities at masses 40, 44, 57 and 61 were recorded. Results of 10 replicate measurements are summarized in Table 2. The ratios of 0.0241 and 0.0249 obtained for $Ca^+$ and $CaOH^+$ species are about 12–16% higher than the accepted ratio of 0.0215 for $^{44}$Ca/$^{40}$Ca. On the per u basis the bias is about 3–4%. Although this mass bias is larger than the per u bias of about 1% for K discussed previously, it is within the range of the mass bias reported in the literature.[8] The discrepancy between the mass bias obtained with K and Ca in this work is probably attributable to the different flames used for the two elements.

The feasibility of using $CaOH^+$ species for isotope ratio analysis was evaluated by comparing the isotope ratio and the ratio precision at $CaOH^+$ masses with those at $Ca^+$ masses. It is expected that the intensity ratio at $CaOH^+$ masses would be identical with that of the corresponding $Ca^+$ masses. The 3% difference between the two ratios in Table 2 is probably due to the mass bias since these ratios are not corrected for

**Table 2** Isotope ratio measurement of a 40 ppm Ca solution

| | Average intensity at mass | | | | Ratio | |
|---|---|---|---|---|---|---|
| | 40 | 44 | 57 | 61 | 44/40[a] | 61/57[a] |
| | 6659 | 160.7 | $8.361 \times 10^4$ | 2085 | $2.41 \times 10^{-2}$ | $2.49 \times 10^{-2}$ |
| RSD (%) | 8 | 9 | 7 | 7 | 3 | 0.5 |

[a]Not corrected for mass bias.

**Table 3** Intensity and the standard deviation ($n = 5$) of K, Na and Ca solutions at Ca and CaOH masses

| Sample[a] | 40 ($^{40}Ca^+$) | 44 ($^{44}Ca^+$) | 57 ($^{40}CaOH^+$) | 61 ($^{44}CaOH^+$) |
|---|---|---|---|---|
| Blank | 1 ± 0.3 | 0.8 ± 0.2 | 4 ± 0.8 | 1 ± 0.4 |
| Ca | 3000 ± 40 | 70 ± 2 | 40000 ± 200 | 900 ± 200 |
| Na | 1 ± 0.3 | 0.9 ± 0.3 | 8 ± 0.7 | 0.8 ± 0.4 |
| Na + Ca | 50 ± 4 | 2 ± 0.5 | 700 ± 10 | 20 ± 2 |
| K | 100 ± 3 | 0.8 ± 0.3 | 3000 ± 20 | 1 ± 0.4 |
| K + Ca | 300 ± 3 | 4 ± 0.9 | 5000 ± 80 | 50 ± 2 |

[a]Na, 100 ppm Na; K, 10 ppm K; Ca, 10 ppm Ca.

the bias. The measured ratio precision of 0.5% RSD at $CaOH^+$ masses is much smaller than the 10% predicted by the law of error propagation with 7% RSD each at masses 57 and 61 (Table 2), suggesting that the intensities at masses 57 and 61 are highly correlated. This high correlation substantiates the viability of using $CaOH^+$ species for isotope ratio analysis. The ratio precision listed in Table 2 is apparently limited by the counting statistics since the total counts measured at each mass are much less than $10^6$. As a result, a better ratio precision was obtained at $CaOH^+$ masses because of the higher sensitivity relative to that at $Ca^+$ masses, thus making $CaOH^+$ the species of choice for isotope ratio measurements.

The effects of easily ionized elements (EIE) Na and K on Ca signal intensities at masses 40, 44, 57 and 61 are summarized in Table 3. The intensities for single element solutions of Na and K are also included. The count rate of 100 and 3000 observed at masses 40 and 57 for the 10 ppm K solution are probably due to $^{40}K^+$ and $^{39}K(H_2O)^+$ species discussed earlier. The ionization suppression from Na and K is evident when the signal from the Ca solution is compared with those with alkali elements in addition. A 60-fold and a 20-fold suppression of Ca signal were observed when 100 ppm Na and 10 ppm K were added to the 10 ppm Ca solution, respectively. In addition to the multiplicative interferences due to ionization suppression, the 10 ppm K in the Ca solution resulted in additive interferences at masses 40 and 57 due to $^{40}K^+$ and $^{39}K(H_2O)^+$ species. A separation may be necessary if Ca is to be determined in high concentrations of easily ionized elements.

## Conclusion

The mass spectral background of the air–hydrogen flame was very simple; however, the analyte spectra were complicated. The low flame temperature relative to an ICP resulted in a limited number of alkali and alkaline earth elements becoming appreciably ionized. The isotope ratio measurement of K and Ca was successfully demonstrated with the FIMS. Two major limitations relative to ICP-MS are severe EIE interferences and the presence of analyte ion-solvent clusters in the spectra. Although the molecular ions complicate the analytical spectra, they can sometimes be used to advantage for elements such as Ca. Compared with the acetylene flame, the air hydrogen flame is equally capable while being more practical as an ion source for FIMS.

## References


1 M. A. Vaughan and G. Horlick, *Appl. Spectrosc.*, 1986, **40**, 434.
2 S. H. Tan and G. Horlick, *Appl. Spectrosc.*, 1986, **40**, 455.
3 A. Montaser, H. Tan, I. Ishii, S. Nam and S. Cai, *Anal. Chem.*, 1991, **63**, 2660.
4 L. C. Alves, D. R. Wiederin and R. S. Houk, *Anal. Chem.*, 1992, **64**, 1164.
5 A. Montaser and H. Zhang, in *Inductively Coupled Plasma Mass Spectrometry*, ed. A. Montaser, Wiley-VCH, New York, 1998.
6 J. W. Lam and J. W. McLaren, *J. Anal. At. Spectrom.*, 1990, **5**, 419.
7 F. G. Smith, D. R. Wiederin and R. S. Houk, *Anal. Chem.*, 1991, **63**, 1458.
8 S. Jiang, R. S. Houk and M. A. Stevens, *Anal. Chem.*, 1988, **60**, 1217.
9 S. D. Tanner, *J. Anal. At. Spectrom.*, 1995, **10**, 905.
10 H. Zhang, S. Nam, M. Cai and A. Montaser, *Appl. Spectrosc.*, 1996, **50**, 427.
11 S. Nam, H. Zhang, M. Cai, J. Lim and A. Montaser, *Fresenius' J. Anal. Chem.*, 1996, **355**, 510.
12 G. C. Eltenton, *J. Chem. Phys.*, 1947, **15**, 455.
13 A. N. Hayhurst and T. M. Sugden, *Proc. R. Soc. London, Ser. A*, 1966, **293**, 36.
14 A. N. Hayhurst, D. B. Kittleson and N. R. Telford, *Combust. Flame*, 1977, **28**, 123.
15 H. E. Taylor, J. Garbarino and S. R. Koirtyohann, *Appl. Spectrosc.*, 1991, **45**, 886.
16 G. C. Turk, L. Yu and S. R. Koirtyohann, *Spectrochim. Acta, Part B*, 1994, **49**, 1537.
17 *Handbook of Flame Spectroscopy*, ed. M. L. Parsons, B. W. Smith and G. E. Bentley, Plenum Press, New York, 1975.
18 *Instrumental Methods of Analysis*, ed. H. H. Willard, L. L. Merritt, Jr and J. A. Dean, 5th edn., Van Nostrand, New York, 1974.
19 D. J. Douglas and J. B. French, *J. Anal. At. Spectrom.*, 1988, **3**, 743.
20 J. A. Green and T. M. Sugden, in *9th International Symposium on Combustion*, ed. W. G. Berl, Academic Press, New York, 1963, pp. 607–621.
21 M. N. Saha, *Philos. Mag.*, 1920, **40**, 472.
22 F. T. Greene and T. A. Milne, *Adv. Mass Spectrom.*, 1964, **3**, 841.
23 D. J. Douglas, in *Inductively Coupled Plasma in Analytical Atomic Spectrometry*, ed. A. Montaser and D. W. Golightly, VCH, New York, 2nd edn., 1992.
24 G. R. Agnes and G. Horlick, *Appl. Spectrosc.*, 1995, **49**, 324.
25 *Perkin-Elmer Technical Summary*, TSMS-12, Perkin-Elmer, Norwalk, CT, 1991.
26 *Nuclear and Radiochemistry*, ed. G. Friedlander, J. W. Henedy, E. S. Macias and J. M. Miller, Wiley, New York, 3rd edn., 1981.
27 J. A. McLean, H. Zhang and A. Montaser, *Anal. Chem.*, 1998, **70**, 1012.


*Paper 8/09797F*